

RECEIVED: May 21, 2024

ACCEPTED: August 22, 2024

PUBLISHED: September 17, 2024

Transverse polarization measurement of Λ hyperons in pNe collisions at $\sqrt{s_{NN}} = 68.4$ GeV with the LHCb detector



The LHCb collaboration

E-mail: camilla.de.angelis@cern.ch

ABSTRACT: A measurement of the transverse polarization of the Λ and $\bar{\Lambda}$ hyperons in $p\text{Ne}$ fixed-target collisions at $\sqrt{s_{NN}} = 68.4$ GeV is presented using data collected by the LHCb detector. The polarization is studied using the decay $\Lambda \rightarrow p\pi^-$ together with its charge conjugated process, the integrated values measured are

$$P_\Lambda = 0.029 \pm 0.019 \text{ (stat)} \pm 0.012 \text{ (syst)},$$

$$P_{\bar{\Lambda}} = 0.003 \pm 0.023 \text{ (stat)} \pm 0.014 \text{ (syst)}.$$

Furthermore, the results are shown as a function of the Feynman x variable, transverse momentum, pseudorapidity and rapidity of the hyperons, and are compared with previous measurements.

KEYWORDS: Fixed Target Experiments, Polarization

ARXIV EPRINT: [2405.11324](https://arxiv.org/abs/2405.11324)

Contents

1	Introduction	1
2	The LHCb detector	2
3	Data sample and analysis strategy	2
4	Simulation and efficiencies	3
5	Results and systematic uncertainties	4
6	Conclusions	7
	The LHCb collaboration	11

1 Introduction

The spontaneous transverse polarization of Λ hyperons, spin 1/2 baryons with a mass of $1115.683 \pm 0.006 \text{ MeV}/c^2$ [1], was first observed in 1976 in unpolarized fixed-target collisions of protons with an energy of 300 GeV and a beryllium target [2]. This result was in contradiction with the expectation that the large number of final states in high-energy particle production would suppress polarization effects and showed that spin effects contribute significantly even at high-energy. A polarizing fragmentation function, denoted by D_{1T}^\perp , has been proposed in refs. [3–5] to account for the polarized production of Λ hyperons. The mechanism involving the D_{1T}^\perp function is the same as that used in the framework of the transverse-momentum-dependent unpolarized fragmentation functions (TMDs) to describe the fragmentation of an unpolarized quark into a transversely polarized hadron. The spin and azimuthal asymmetries observed at sufficiently large energy scales cannot be explained by asymmetries at the level of the hard partonic process, instead their origin must lie in soft processes. By maintaining an explicit dependence on the intrinsic partonic motion, TMDs account for spin and momentum correlations at the soft level, potentially explaining the observed asymmetries. Since these functions arise from soft mechanisms, they are difficult to calculate from first principles. Hence, just as with collinear parton distribution functions and fragmentation functions, one possible approach is to determine them from experimental data. Several attempts were made to describe Λ polarization, both on the theoretical and experimental sides, at different accelerators and center-of-mass energies. Particularly relevant are the measurements from the STAR experiment at RHIC [6] and Belle at KEKB [7]. None of these results led to a fully satisfactory answer, and the mechanism giving rise to Λ polarization is still unclear. In this paper, a measurement of transverse Λ and $\bar{\Lambda}$ polarization is presented, using the LHCb experiment in a fixed-target configuration. The polarization is determined using proton-neon ($p\text{Ne}$) data collected in 2017 from collisions at a nucleon-nucleon center-of-mass energy of $\sqrt{s_{\text{NN}}} = 68.4 \text{ GeV}$, generated by a 2.5 TeV proton beam incident on neon nuclei

at rest and corresponding to an integrated luminosity of 24.9 nb^{-1} . The hyperons are reconstructed through the decays $\Lambda \rightarrow p\pi^-$ and $\bar{\Lambda} \rightarrow \bar{p}\pi^+$. The results are obtained as a function of the transverse momentum (p_T) of the hyperon, the pseudorapidity (η), the rapidity (y) and the Feynman variable $x_F = \frac{2 \cdot p_L}{\sqrt{s_{NN}}}$ (where p_L is the longitudinal momentum of the particle), as a non trivial dependence of the polarization on these variables has been reported in other publications [8].

2 The LHCb detector

The LHCb detector [9, 10] is a single-arm forward spectrometer, designed for the study of particles containing c or b quarks, covering the pseudorapidity range $2 < \eta < 5$. The detector includes: a silicon-strip vertex locator (VELO), three tracking stations of silicon-strip detectors and straw drift tubes, two ring-imaging Cherenkov detectors (RICH) that are able to discriminate between different species of charged hadrons, a calorimeter system consisting of scintillating-pad and preshower detectors, electromagnetic and hadronic calorimeters, and a muon detector composed of alternating layers of iron and multiwire proportional chambers. The System for Measuring the Overlap with Gas (SMOG) [11] enables the injection of gases with a pressure of $\mathcal{O}(10^{-7})$ mbar in the beam pipe section inside the VELO, allowing LHCb to operate as a fixed-target experiment. The SMOG system thus provides a unique opportunity to study proton-nucleus and nucleus-nucleus collisions with various gaseous targets using the LHC beams. In this configuration, the LHCb acceptance extends to the negative rapidity hemisphere, due to the boost induced by the high-energy proton beam, which points to the positive- z direction.

3 Data sample and analysis strategy

The $p\text{Ne}$ sample was taken during the pp data-taking period. Fixed-target events were collected only when a bunch in the beam pointing towards the LHCb detector crossed the interaction region without a corresponding bunch in the beam pointing to the opposite direction. To suppress the remaining pp background, the z -coordinate of the $p\text{Ne}$ primary vertex (PV) is required to lie in the fiducial region $z_{\text{PV}} \in [-200, -100] \cup [100, 150] \text{ mm}$.¹ Furthermore, events with more than four hits in the VELO stations upstream of the interaction region are rejected. The online event selection is performed by a trigger [12], that requires at least one track reconstructed in the VELO. Since the Λ reconstruction requires two tracks, this trigger condition does not bias the measurement. In the offline selection, the Λ candidates are required to be reconstructed from proton and pion tracks with opposite charge, forming a vertex with a good-quality fit. Protons and pions are required to have a minimum transverse momentum of $100 \text{ MeV}/c$ and a minimum momentum of $2 \text{ GeV}/c$. Particle identification (PID) requirements based on the information from the RICH detectors are applied to select protons. Finally, to suppress the contribution of nonprompt Λ hyperons, the impact parameter of the Λ candidate with respect to the PV is required to be less than 1.5 mm , which reduces this contribution to about 5%. Figure 1 shows the $p\pi^-$ and $\bar{p}\pi^+$ invariant-mass distributions obtained after all the selection criteria have been applied. The distributions are fitted with

¹ $z_{\text{PV}} = 0$ is the z coordinate of the center of the pp interaction region.

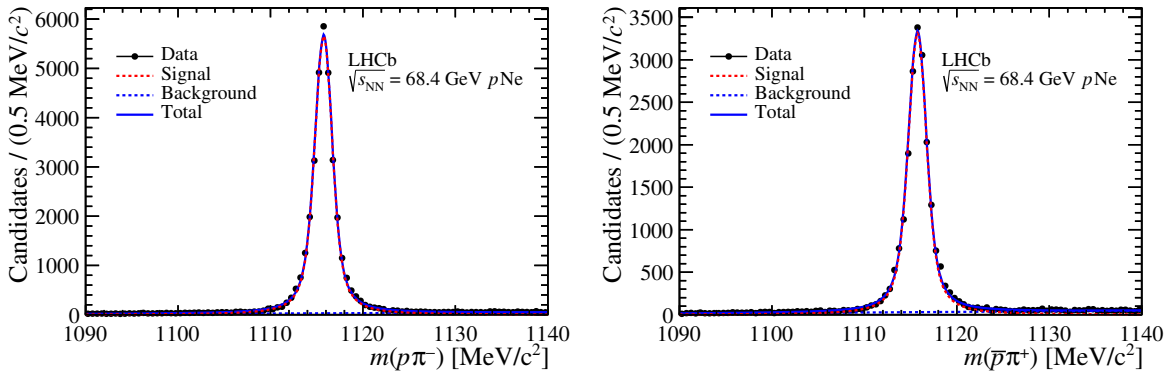


Figure 1. Invariant-mass distributions for (left) Λ and (right) $\bar{\Lambda}$ candidates after all selection requirements are applied. The fit result is overlaid on the data.

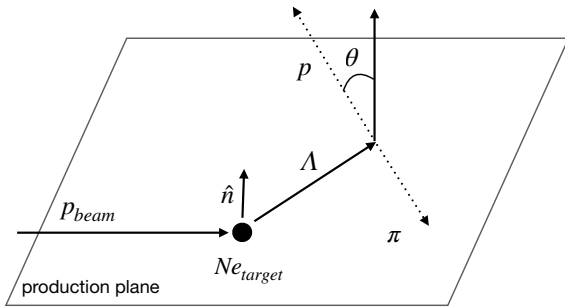


Figure 2. Sketch of the Λ production and decay. The polarization vector \hat{P}_Λ is aligned with the normal vector \hat{n} to the Λ production plane; θ is the angle between the momentum of the decay proton and \hat{n} in the Λ rest frame.

the convolution of a Cauchy and a Gaussian function to describe the signal shape and a first-order polynomial to model the background.

The decays $\Lambda \rightarrow p\pi^-$ and $\bar{\Lambda} \rightarrow \bar{p}\pi^+$ exhibit significant parity violation, resulting in large asymmetries in the angular distribution of their decay particles. In particular, the angular distribution of the proton in the Λ rest frame is given by

$$\frac{dN}{d\cos\theta} = \frac{dN_0}{d\cos\theta}(1 + \alpha P_\Lambda \cos\theta), \quad (3.1)$$

where θ is the angle between the proton momentum and the normal (\hat{n}) to the production plane spanned by the beam and the Λ momentum directions as sketched in figure 2, $\frac{dN_0}{d\cos\theta}$ is the decay distribution for unpolarized Λ hyperons, P_Λ is the magnitude of the Λ polarization, and α is the value of the parity-violating decay asymmetry for the channel under study of the Λ hyperon. The magnitude of the polarization is determined from a fit to the angular distribution of the proton in 10 bins of $\cos\theta$.

4 Simulation and efficiencies

Efficiencies are estimated using samples of fully simulated events. The simulated decays are reconstructed and analyzed using the same software tools as those used to process

the data. In the simulation, Λ hyperons are generated using PYTHIA [13] with a specific LHCb configuration [14] and with colliding-proton beam momentum equal to the momentum per nucleon of the beam and target in the centre-of-mass frame. The decays of unstable particles are described by EVTGEN [15], in which final-state radiation is generated using PHOTOS [16]. The four-momentum of the Λ decay particles is then embedded into $p\text{Ne}$ minimum bias events that are generated with the EPOS event generator [17]. The interaction of the generated particles with the detector and its response are implemented using the GEANT4 toolkit [18, 19] as described in ref. [20].

After reconstruction, the simulated samples are weighted to improve agreement with data. Weights are calculated as the ratio between the normalized data and simulated distributions as a function of p_{T} , η and z_{PV} with

$$w(p_{\text{T}}, \eta, z_{\text{PV}}) = w(p_{\text{T}}, \eta) \cdot w(z_{\text{PV}}), \quad (4.1)$$

where $w(p_{\text{T}}, \eta)$ is evaluated in 6 intervals of transverse momentum between 300 and 2500 MeV/ c and 7 intervals of pseudorapidity between 2 and 5. The weights $w(z_{\text{PV}})$ are evaluated in 6 intervals between -200 and 150 mm, ignoring the region between -100 and 100 mm outside the fiducial region considered in the analysis. Through the weighting procedure, the simulation is corrected on average by 6% as a function of transverse momentum and pseudorapidity, and by 4% as a function of z_{PV} , for both Λ and $\bar{\Lambda}$ hyperons. Accounting for efficiency factors, eq. (3.1) is modified to

$$\frac{dN}{d \cos \theta} = \frac{dN_0}{d \cos \theta} (1 + \alpha P_{\Lambda} \cos \theta) \times \epsilon(\cos \theta) \times \epsilon_{\text{PID}}, \quad (4.2)$$

where ϵ_{PID} is the particle identification efficiency for the protons, estimated from dedicated calibration data samples and computed as a function of the proton kinematics. The $\epsilon(\cos \theta)$ term is the product of acceptance, reconstruction and selection efficiencies. It is determined using simulation as $\epsilon(\cos \theta) = f_{\text{rec}}(\cos \theta)/f_{\text{gen}}(\cos \theta)$, where f indicates the $\cos \theta$ distribution for generated candidates (f_{gen}), without any detector effect, or for fully reconstructed candidates (f_{rec}), with detector effects included. As the polarization effects are not included in the simulation, the generated $\cos \theta$ distribution is uniform. Since only the shape of the distribution is relevant, the efficiency is proportional to the reconstructed $\cos \theta$ distributions, and the generated one is ignored. To correct the angular distributions in data, in each $\cos \theta$ bin, the normalized number of candidates in the data is divided by the normalized number of candidates in the simulated reconstructed sample.

5 Results and systematic uncertainties

The proton angular distributions, after efficiency correction, are shown in figure 3. The function $f(\cos \theta) = A(1 + \alpha P_{\Lambda} \cos \theta)$ is fitted to the data distributions, where $\alpha = 0.746 \pm 0.007$ for Λ and $\alpha = -0.757 \pm 0.004$ for $\bar{\Lambda}$ are fixed to their world average value [1]. The magnitude of the polarization is given by the free parameter of the fit shown in figure 3.

Several sources of systematic uncertainties are considered. The fit to the invariant-mass distribution is repeated using a double-sided Crystal Ball function [21] instead of the convolution of a Cauchy and a Gaussian function for the signal shape, and a second-order

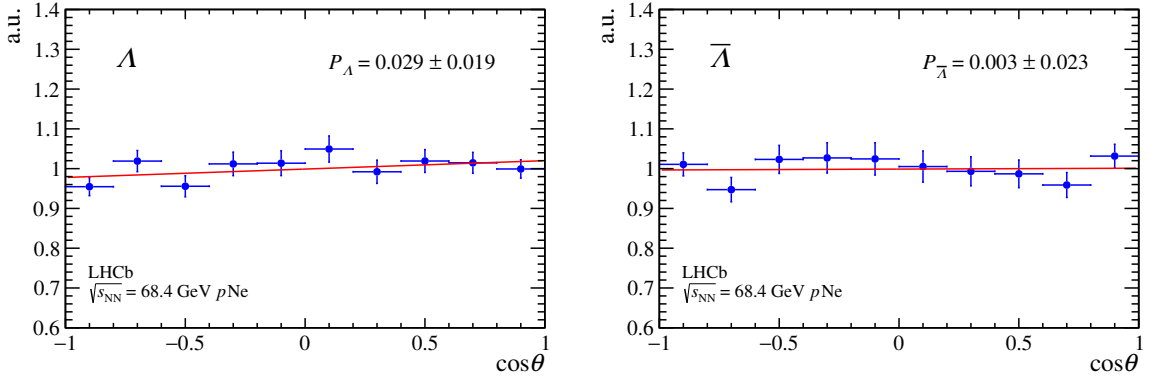


Figure 3. Efficiency-corrected $\cos \theta$ distributions, for (left) Λ and (right) $\bar{\Lambda}$ hyperons. The result of the fit is overlaid (red line).

polynomial instead of a first-order one for the background, and the values of the polarization are determined again. The systematic uncertainty is determined as the deviations of these results with respect to those of the default fit. Uncertainties related to the weighting procedure applied to the simulation are taken into consideration by carrying out 100 trials, randomly varying each weight within its uncertainty, calculating new values for the polarization, and taking as systematic uncertainty the largest difference in the polarization values compared to the default one. The choice of the variables used to weight the simulation is also considered; the uncertainty is calculated as the difference between the results obtained by using the track multiplicity and those obtained using the Λ pseudorapidity in the calculation of the weights. The choice of binning for the angular distributions affects the fit results. This is taken into account by repeating the polarization measurements using 5 bins instead of 10 in the angular distribution. Another contribution is associated with the estimation of PID efficiencies. An alternative approach is used, where the particle identification efficiencies are directly estimated from the simulation rather than using dedicated calibration samples. Another systematic uncertainty contribution arises from nonprompt Λ hyperon contamination in the data sample, which is estimated from simulation to account for 5% of the total yield. To estimate an upper limit on the nonprompt contamination, the impact parameter requirement (which retains approximately 50% of the nonprompt signal) is removed, the measurement is repeated and the difference with the baseline value is taken as systematic uncertainty. The systematic uncertainty due to the external parameter α is found to be negligible. The total systematic uncertainty is computed as the sum in quadrature of each contribution shown in table 1. The systematic contributions are found to be small and the measurement is dominated by statistical uncertainties. The statistical effect on each systematic contribution is not negligible as reflected in the differences between Λ and $\bar{\Lambda}$ hyperons. The final polarization measurements are

$$P_\Lambda = 0.029 \pm 0.019 \text{ (stat)} \pm 0.012 \text{ (syst)},$$

$$P_{\bar{\Lambda}} = 0.003 \pm 0.023 \text{ (stat)} \pm 0.014 \text{ (syst)}.$$

The polarization measurements have also been performed in bins of p_T , η , y and x_F . The results are shown in figure 4 and listed in table 2. Other experiments with different energies

Source	Λ	$\bar{\Lambda}$
Signal estimation	0.007	0.001
Background estimation	0.001	0.010
Kinematic weights	0.001	0.001
Multiplicity dependence	0.001	0.004
Binning of $\cos \theta$ distributions	0.007	0.006
PID efficiencies	0.002	0.005
Nonprompt contamination	0.005	0.002

Table 1. Contributions of systematic uncertainties on the polarization measurement for Λ and $\bar{\Lambda}$ hyperons.

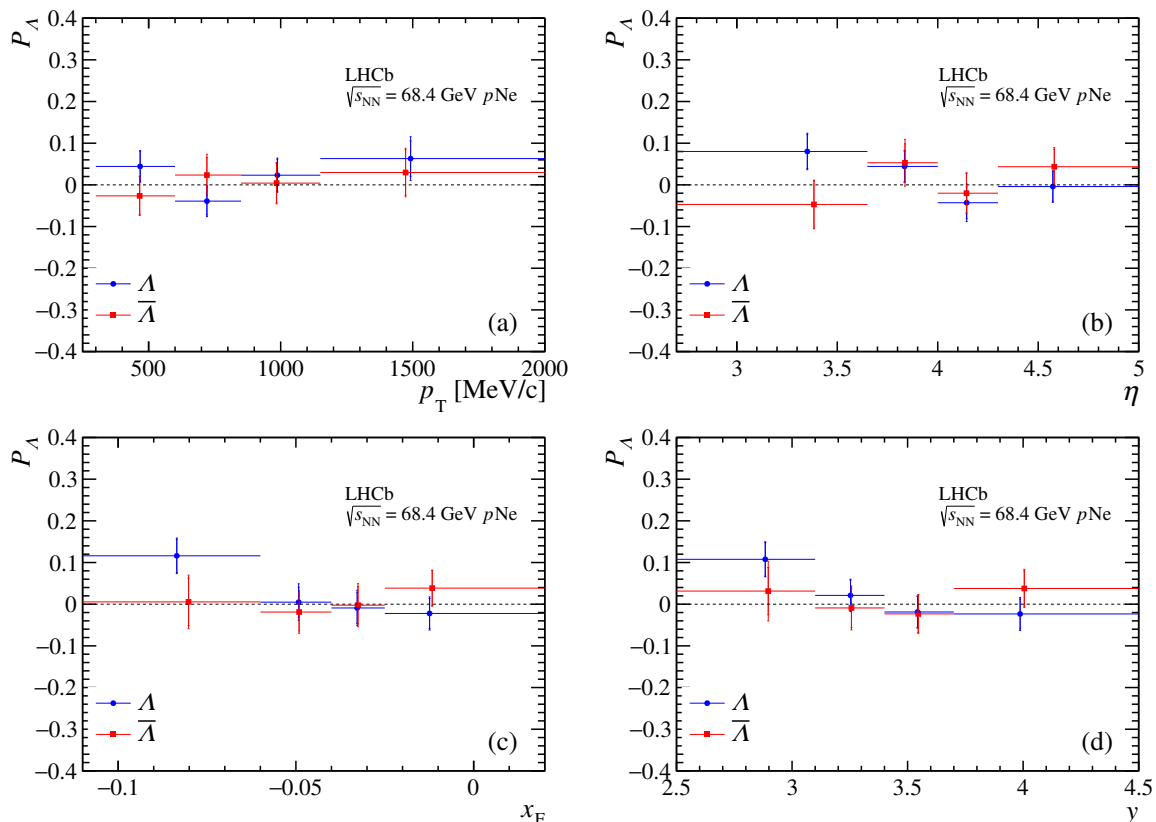


Figure 4. Polarization as a function of (a) p_T , (b) η , (c) x_F and (d) y . Blue (red) symbols are for Λ ($\bar{\Lambda}$). In each plot the data is integrated over the $0.3 < p_T < 3$ GeV/c and/or $2 < \eta < 5$ kinematic range.

and collision systems have measured the Λ polarization. In its fixed-target configuration, the LHCb experiment covers an energy and kinematic range that is largely unexplored. Figure 5 compares and shows the agreement between the results of this paper with measurements from other experiments, including ATLAS [22], an experiment at the M2 beam-line at Fermilab [23], the E799 experiment [24], NA48 [25], and HERA-B [26]. The measurements reported here, and those from HERA-B, cover negative values of x_F , so the results are first transformed

	P_Λ	$P_{\bar{\Lambda}}$
p_T [MeV/c]		
[300, 600]	$0.044 \pm 0.035 \pm 0.013$	$-0.026 \pm 0.044 \pm 0.015$
[600, 850]	$-0.039 \pm 0.033 \pm 0.016$	$0.023 \pm 0.042 \pm 0.027$
[850, 1150]	$0.023 \pm 0.038 \pm 0.015$	$0.004 \pm 0.047 \pm 0.015$
[1150, 3000]	$0.063 \pm 0.042 \pm 0.031$	$0.029 \pm 0.054 \pm 0.021$
η		
[2.00, 3.65]	$0.080 \pm 0.040 \pm 0.016$	$-0.047 \pm 0.057 \pm 0.011$
[3.65, 4.00]	$0.044 \pm 0.036 \pm 0.012$	$0.053 \pm 0.045 \pm 0.033$
[4.00, 4.30]	$-0.043 \pm 0.038 \pm 0.024$	$-0.020 \pm 0.047 \pm 0.014$
[4.30, 5.00]	$-0.004 \pm 0.035 \pm 0.014$	$0.043 \pm 0.042 \pm 0.020$
x_F		
[-0.250, -0.060]	$0.116 \pm 0.040 \pm 0.015$	$0.006 \pm 0.057 \pm 0.030$
[-0.060, -0.040]	$0.005 \pm 0.036 \pm 0.025$	$-0.018 \pm 0.045 \pm 0.023$
[-0.040, -0.025]	$-0.009 \pm 0.037 \pm 0.020$	$0.002 \pm 0.045 \pm 0.026$
[-0.025, 0.100]	$-0.022 \pm 0.036 \pm 0.017$	$0.038 \pm 0.042 \pm 0.008$
y		
[2.0, 3.1]	$0.107 \pm 0.040 \pm 0.011$	$0.031 \pm 0.057 \pm 0.044$
[3.1, 3.4]	$0.021 \pm 0.036 \pm 0.013$	$-0.009 \pm 0.046 \pm 0.025$
[3.4, 3.7]	$-0.019 \pm 0.037 \pm 0.010$	$-0.023 \pm 0.045 \pm 0.013$
[3.7, 5.0]	$-0.023 \pm 0.036 \pm 0.016$	$0.038 \pm 0.042 \pm 0.018$

Table 2. Polarization in bins of p_T , η , x_F , and y for Λ and $\bar{\Lambda}$. The first uncertainties are statistical and the second are systematic.

using the following symmetry of the transverse polarization $P_\Lambda(-x_F) = -P_\Lambda(x_F)$, and then compared with the other measurements.

6 Conclusions

A measurement of transverse polarization of Λ and $\bar{\Lambda}$ hyperons in $p\text{Ne}$ collisions at $\sqrt{s_{\text{NN}}} = 68.4$ GeV by the LHCb experiment is presented. This analysis exploits the innovative and unique fixed-target apparatus at LHC. The measurement in a new collision system and region of phase space can provide additional insights on the mechanism of Λ polarization, which can still not be calculated in quantum chromodynamics. The polarization is measured through the decay $\Lambda \rightarrow p\pi^-$ and its charge conjugate, and is studied both as integrated values and in different bins of four kinematic variables: p_T , η , x_F , and y .

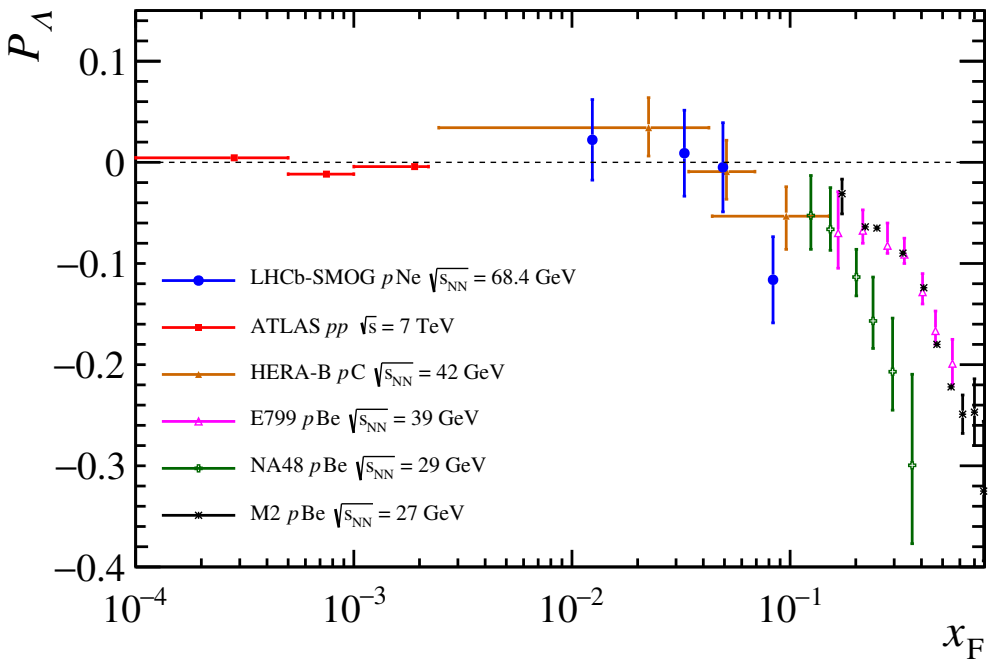


Figure 5. Comparison of polarization as a function of x_F for Λ hyperons obtained in experiments with different energies and with different colliding systems.

The integrated results are

$$P_\Lambda = 0.029 \pm 0.019 \text{ (stat)} \pm 0.012 \text{ (syst)}, \\ P_{\bar{\Lambda}} = 0.003 \pm 0.023 \text{ (stat)} \pm 0.014 \text{ (syst)}.$$

The polarization values obtained in this analysis are compatible with previous measurements, in particular with the HERA-B results which cover a similar x_F interval. The agreement is noteworthy considering the different experiments and colliding systems.

The LHCb fixed-target program has become particularly active since the installation of the SMOG2 system, which increases data luminosity by more than two orders of magnitude compared to the SMOG system used in this analysis. With the new data, we expect to explore different target species and improve our reach into the lower negative regions of x_F which have been poorly explored so far.

Acknowledgments

We thank Umberto D'Alesio for the fruitful discussions. We express our gratitude to our colleagues in the CERN accelerator departments for the excellent performance of the LHC. We thank the technical and administrative staff at the LHCb institutes. We acknowledge support from CERN and from the national agencies: CAPES, CNPq, FAPERJ and FINEP (Brazil); MOST and NSFC (China); CNRS/IN2P3 (France); BMBF, DFG and MPG (Germany); INFN (Italy); NWO (The Netherlands); MNiSW and NCN (Poland); MCID/IFA (Romania); MICINN (Spain); SNSF and SER (Switzerland); NASU (Ukraine); STFC (United Kingdom);

DOE NP and NSF (U.S.A.). We acknowledge the computing resources that are provided by CERN, IN2P3 (France), KIT and DESY (Germany), INFN (Italy), SURF (The Netherlands), PIC (Spain), GridPP (United Kingdom), CSCS (Switzerland), IFIN-HH (Romania), CBPF (Brazil), and Polish WLCG (Poland). We are indebted to the communities behind the multiple open-source software packages on which we depend. Individual groups or members have received support from ARC and ARDC (Australia); Key Research Program of Frontier Sciences of CAS, CAS PIFI, CAS CCEPP, Fundamental Research Funds for the Central Universities, and Sci. & Tech. Program of Guangzhou (China); Minciencias (Colombia); EPLANET, Marie Skłodowska-Curie Actions, ERC and NextGenerationEU (European Union); A*MIDEX, ANR, IPhU and Labex P2IO, and Région Auvergne-Rhône-Alpes (France); AvH Foundation (Germany); ICSC (Italy); GVA, XuntaGal, GENCAT, Inditex, InTalent and Prog. Atracción Talento, CM (Spain); SRC (Sweden); the Leverhulme Trust, the Royal Society and UKRI (United Kingdom).

Open Access. This article is distributed under the terms of the Creative Commons Attribution License ([CC-BY4.0](#)), which permits any use, distribution and reproduction in any medium, provided the original author(s) and source are credited.

References

- [1] PARTICLE DATA collaboration, *Review of Particle Physics*, *Prog. Theor. Exp. Phys.* **2022** (2022) 083C01 [[INSPIRE](#)].
- [2] G. Bunce et al., Λ^0 Hyperon Polarization in Inclusive Production by 300 GeV Protons on Beryllium, *Phys. Rev. Lett.* **36** (1976) 1113 [[INSPIRE](#)].
- [3] D. Boer, C.J. Bomhof, D.S. Hwangs and P.J. Mulders, Spin asymmetries in jet-hyperon production at LHC, *Phys. Lett. B* **659** (2008) 127 [[arXiv:0709.1087](#)] [[INSPIRE](#)].
- [4] D. Boer, Transverse Lambda Polarization at LHC, in the proceedings of the 17th International Workshop on Deep-Inelastic Scattering and Related Subjects, Madrid, Spain, 26–30 April 2009, [arXiv:0907.1610](#) [[INSPIRE](#)].
- [5] P.J. Mulders and R.D. Tangerman, The Complete tree level result up to order $1/Q$ for polarized deep inelastic leptoproduction, *Nucl. Phys. B* **461** (1996) 197 [[hep-ph/9510301](#)] [[INSPIRE](#)].
- [6] T. Gao, Measurement of transverse polarization of $\Lambda/\bar{\Lambda}$ within jet in pp collisions at STAR, *PoS SPIN2023* (2024) 031 [[arXiv:2402.01168](#)] [[INSPIRE](#)].
- [7] BELLE collaboration, Observation of Transverse $\Lambda/\bar{\Lambda}$ Hyperon Polarization in e^+e^- Annihilation at Belle, *Phys. Rev. Lett.* **122** (2019) 042001 [[arXiv:1808.05000](#)] [[INSPIRE](#)].
- [8] HERMES collaboration, Transverse polarization of Λ hyperons from quasireal photoproduction on nuclei, *Phys. Rev. D* **90** (2014) 072007 [[arXiv:1406.3236](#)] [[INSPIRE](#)].
- [9] LHCb collaboration, The LHCb Detector at the LHC, 2008 *JINST* **3** S08005 [[INSPIRE](#)].
- [10] LHCb collaboration, LHCb Detector Performance, *Int. J. Mod. Phys. A* **30** (2015) 1530022 [LHCb-DP-2014-002] [CERN-PH-EP-2014-290] [[arXiv:1412.6352](#)] [[INSPIRE](#)].
- [11] LHCb collaboration, Precision luminosity measurements at LHCb, 2014 *JINST* **9** P12005 [LHCb-PAPER-2014-047] [CERN-PH-EP-2014-221] [[arXiv:1410.0149](#)] [[INSPIRE](#)].

- [12] R. Aaij et al., *The LHCb Trigger and its Performance in 2011, 2013* *JINST* **8** P04022 [LHCb-DP-2012-004] [[arXiv:1211.3055](#)] [[INSPIRE](#)].
- [13] T. Sjöstrand, S. Mrenna and P.Z. Skands, *A Brief Introduction to PYTHIA 8.1*, *Comput. Phys. Commun.* **178** (2008) 852 [[arXiv:0710.3820](#)] [[INSPIRE](#)].
- [14] I. Belyaev et al., *Handling of the generation of primary events in Gauss, the LHCb simulation framework*, *J. Phys. Conf. Ser.* **331** (2011) 032047 [[INSPIRE](#)].
- [15] D.J. Lange, *The EvtGen particle decay simulation package*, *Nucl. Instrum. Meth. A* **462** (2001) 152 [[INSPIRE](#)].
- [16] P. Golonka and Z. Was, *PHOTOS Monte Carlo: A Precision tool for QED corrections in Z and W decays*, *Eur. Phys. J. C* **45** (2006) 97 [[hep-ph/0506026](#)] [[INSPIRE](#)].
- [17] T. Pierog, I. Karpenko, J.M. Katzy, E. Yatsenko and K. Werner, *EPOS LHC: Test of collective hadronization with data measured at the CERN Large Hadron Collider*, *Phys. Rev. C* **92** (2015) 034906 [[arXiv:1306.0121](#)] [[INSPIRE](#)].
- [18] GEANT4 collaboration, *GEANT4 — a simulation toolkit*, *Nucl. Instrum. Meth. A* **506** (2003) 250 [[INSPIRE](#)].
- [19] J. Allison et al., *GEANT4 developments and applications*, *IEEE Trans. Nucl. Sci.* **53** (2006) 270 [[INSPIRE](#)].
- [20] M. Clemencic et al., *The LHCb simulation application, Gauss: Design, evolution and experience*, *J. Phys. Conf. Ser.* **331** (2011) 032023 [[INSPIRE](#)].
- [21] T. Skwarnicki, *A study of the radiative CASCADE transitions between the Upsilon-Prime and Upsilon resonances*, Ph.D. Thesis, Institute of Nuclear Physics, Krakow, Poland (1986) [[INSPIRE](#)].
- [22] ATLAS collaboration, *Measurement of the transverse polarization of Λ and $\bar{\Lambda}$ hyperons produced in proton-proton collisions at $\sqrt{s} = 7$ TeV using the ATLAS detector*, *Phys. Rev. D* **91** (2015) 032004 [[arXiv:1412.1692](#)] [[INSPIRE](#)].
- [23] B. Lundberg et al., *Polarization in Inclusive Λ and $\bar{\Lambda}$ Production at Large p_T* , *Phys. Rev. D* **40** (1989) 3557 [[INSPIRE](#)].
- [24] E.J. Ramberg et al., *Polarization of Lambda and anti-Lambda produced by 800 GeV protons*, *Phys. Lett. B* **338** (1994) 403 [[INSPIRE](#)].
- [25] NA48 collaboration, *A measurement of the transverse polarization of Lambda hyperons produced in inelastic pN-reactions at 450 GeV proton energy*, *Nucl. Phys. B Proc. Suppl.* **75** (1999) 45 [[INSPIRE](#)].
- [26] HERA-B collaboration, *Polarization of Λ and $\bar{\Lambda}$ in 920 GeV fixed-target proton-nucleus collisions*, *Phys. Lett. B* **638** (2006) 415 [[hep-ex/0603047](#)] [[INSPIRE](#)].

The LHCb collaboration

- R. Aaij ID^{36} , A.S.W. Abdelmotteleb ID^{55} , C. Abellan Beteta 49 , F. Abudinén ID^{55} , T. Ackernley ID^{59} , A.A. Adefisoye ID^{67} , B. Adeva ID^{45} , M. Adinolfi ID^{53} , P. Adlarson ID^{79} , C. Agapopoulou ID^{13} , C.A. Aidala ID^{80} , Z. Ajaltouni 11 , S. Akar ID^{64} , K. Akiba ID^{36} , P. Albicocco ID^{26} , J. Albrecht ID^{18} , F. Alessio ID^{47} , M. Alexander ID^{58} , Z. Aliouche ID^{61} , P. Alvarez Cartelle ID^{54} , R. Amalric ID^{15} , S. Amato ID^3 , J.L. Amey ID^{53} , Y. Amhis $\text{ID}^{13,47}$, L. An ID^6 , L. Anderlini ID^{25} , M. Andersson ID^{49} , A. Andreianov ID^{42} , P. Andreola ID^{49} , M. Andreotti ID^{24} , D. Andreou ID^{67} , A. Anelli $\text{ID}^{29,p}$, D. Ao ID^7 , F. Archilli $\text{ID}^{35,v}$, M. Argenton ID^{24} , S. Arguedas Cuendis ID^9 , A. Artamonov ID^{42} , M. Artuso ID^{67} , E. Aslanides ID^{12} , R. Ataide Da Silva ID^{48} , M. Atzeni ID^{63} , B. Audurier ID^{14} , D. Bacher ID^{62} , I. Bachiller Perea ID^{10} , S. Bachmann ID^{20} , M. Bachmayer ID^{48} , J.J. Back ID^{55} , P. Baladron Rodriguez ID^{45} , V. Balagura ID^{14} , W. Baldini ID^{24} , H. Bao ID^7 , J. Baptista de Souza Leite ID^{59} , M. Barbetti $\text{ID}^{25,m}$, I.R. Barbosa ID^{68} , R.J. Barlow ID^{61} , M. Barnyakov ID^{23} , S. Barsuk ID^{13} , W. Barter ID^{57} , M. Bartolini ID^{54} , J. Bartz ID^{67} , J.M. Basels ID^{16} , G. Bassi ID^{33} , B. Batsukh ID^5 , A. Bay ID^{48} , A. Beck ID^{55} , M. Becker ID^{18} , F. Bedeschi ID^{33} , I.B. Bediaga ID^2 , S. Belin ID^{45} , V. Bellee ID^{49} , K. Belous ID^{42} , I. Belov ID^{27} , I. Belyaev ID^{34} , G. Benane ID^{12} , G. Bencivenni ID^{26} , E. Ben-Haim ID^{15} , A. Berezhnoy ID^{42} , R. Bernet ID^{49} , S. Bernet Andres ID^{43} , A. Bertolin ID^{31} , C. Betancourt ID^{49} , F. Betti ID^{57} , J. Bex ID^{54} , Ia. Bezshyiko ID^{49} , J. Bhom ID^{39} , M.S. Bieker ID^{18} , N.V. Biesuz ID^{24} , P. Billoir ID^{15} , A. Biolchini ID^{36} , M. Birch ID^{60} , F.C.R. Bishop ID^{10} , A. Bitadze ID^{61} , A. Bizzeti ID , T. Blake ID^{55} , F. Blanc ID^{48} , J.E. Blank ID^{18} , S. Blusk ID^{67} , V. Bocharkov ID^{42} , J.A. Boelhauve ID^{18} , O. Boente Garcia ID^{14} , T. Boettcher ID^{64} , A. Bohare ID^{57} , A. Boldyrev ID^{42} , C.S. Bolognani ID^{76} , R. Bolzonella $\text{ID}^{24,l}$, N. Bondar ID^{42} , F. Borgato $\text{ID}^{31,q}$, S. Borghi ID^{61} , M. Borsato $\text{ID}^{29,p}$, J.T. Borsuk ID^{39} , S.A. Bouchiba ID^{48} , T.J.V. Bowcock ID^{59} , A. Boyer ID^{47} , C. Bozzi ID^{24} , A. Brea Rodriguez ID^{48} , N. Breer ID^{18} , J. Brodzicka ID^{39} , A. Brossa Gonzalo ID^{45} , J. Brown ID^{59} , D. Brundu ID^{30} , E. Buchanan 57 , A. Buonaura ID^{49} , L. Buonincontri $\text{ID}^{31,q}$, A.T. Burke ID^{61} , C. Burr ID^{47} , A. Butkevich ID^{42} , J.S. Butter ID^{54} , J. Buytaert ID^{47} , W. Byczynski ID^{47} , S. Cadeddu ID^{30} , H. Cai 72 , R. Calabrese $\text{ID}^{24,l}$, S. Calderon Ramirez ID^9 , L. Calefice ID^{44} , S. Cali ID^{26} , M. Calvi $\text{ID}^{29,p}$, M. Calvo Gomez ID^{43} , P. Camargo Magalhaes $\text{ID}^{2,z}$, J.I. Cambon Bouzas ID^{45} , P. Campana ID^{26} , D.H. Campora Perez ID^{76} , A.F. Campoverde Quezada ID^7 , S. Capelli ID^{29} , L. Capriotti ID^{24} , R. Caravaca-Mora ID^9 , A. Carbone $\text{ID}^{23,j}$, L. Carcedo Salgado ID^{45} , R. Cardinale $\text{ID}^{27,n}$, A. Cardini ID^{30} , P. Carniti $\text{ID}^{29,p}$, L. Carus 20 , A. Casais Vidal ID^{63} , R. Caspary ID^{20} , G. Casse ID^{59} , J. Castro Godinez ID^9 , M. Cattaneo ID^{47} , G. Cavallero $\text{ID}^{24,47}$, V. Cavallini $\text{ID}^{24,l}$, S. Celani ID^{20} , D. Cervenkov ID^{62} , S. Cesare $\text{ID}^{28,o}$, A.J. Chadwick ID^{59} , I. Chahroud ID^{80} , M. Charles ID^{15} , Ph. Charpentier ID^{47} , E. Chatzianagnostou ID^{36} , C.A. Chavez Barajas ID^{59} , M. Chefdeville ID^{10} , C. Chen ID^{12} , S. Chen ID^5 , Z. Chen ID^7 , A. Chernov ID^{39} , S. Chernyshenko ID^{51} , V. Chobanova ID^{78} , S. Cholak ID^{48} , M. Chrzaszcz ID^{39} , A. Chubykin ID^{42} , V. Chulikov ID^{42} , P. Ciambrone ID^{26} , X. Cid Vidal ID^{45} , G. Ciezarek ID^{47} , P. Cifra ID^{47} , P.E.L. Clarke ID^{57} , M. Clemencic ID^{47} , H.V. Cliff ID^{54} , J. Closier ID^{47} , C. Cocha Toapaxi ID^{20} , V. Coco ID^{47} , J. Cogan ID^{12} , E. Cogneras ID^{11} , L. Cojocariu ID^{41} , P. Collins ID^{47} , T. Colombo ID^{47} , A. Comerma-Montells ID^{44} , L. Congedo ID^{22} , A. Contu ID^{30} , N. Cooke ID^{58} , I. Corredoira ID^{45} , A. Correia ID^{15} , G. Corti ID^{47} , J.J. Cottee Meldrum 53 , B. Couturier ID^{47} , D.C. Craik ID^{49} , M. Cruz Torres $\text{ID}^{2,g}$, E. Curras Rivera ID^{48} , R. Currie ID^{57} , C.L. Da Silva ID^{66} , S. Dadabaev ID^{42} , L. Dai ID^{69} , X. Dai ID^6 , E. Dall'Occo ID^{18} , J. Dalseno ID^{45} , C. D'Ambrosio ID^{47} , J. Daniel ID^{11} , A. Danilina ID^{42} , P. d'Argent ID^{22} , A. Davidson ID^{55} ,

- J.E. Davies $\textcolor{blue}{D}^{61}$, A. Davis $\textcolor{blue}{D}^{61}$, O. De Aguiar Francisco $\textcolor{blue}{D}^{61}$, C. De Angelis $\textcolor{blue}{D}^{30,k}$, F. De Benedetti $\textcolor{blue}{D}^{47}$, J. de Boer $\textcolor{blue}{D}^{36}$, K. De Bruyn $\textcolor{blue}{D}^{75}$, S. De Capua $\textcolor{blue}{D}^{61}$, M. De Cian $\textcolor{blue}{D}^{20,47}$, U. De Freitas Carneiro Da Graca $\textcolor{blue}{D}^{2,b}$, E. De Lucia $\textcolor{blue}{D}^{26}$, J.M. De Miranda $\textcolor{blue}{D}^2$, L. De Paula $\textcolor{blue}{D}^3$, M. De Serio $\textcolor{blue}{D}^{22,h}$, P. De Simone $\textcolor{blue}{D}^{26}$, F. De Vellis $\textcolor{blue}{D}^{18}$, J.A. de Vries $\textcolor{blue}{D}^{76}$, F. Debernardis $\textcolor{blue}{D}^{22}$, D. Decamp $\textcolor{blue}{D}^{10}$, V. Dedu $\textcolor{blue}{D}^{12}$, L. Del Buono $\textcolor{blue}{D}^{15}$, B. Delaney $\textcolor{blue}{D}^{63}$, H.-P. Dembinski $\textcolor{blue}{D}^{18}$, J. Deng $\textcolor{blue}{D}^8$, V. Denysenko $\textcolor{blue}{D}^{49}$, O. Deschamps $\textcolor{blue}{D}^{11}$, F. Dettori $\textcolor{blue}{D}^{30,k}$, B. Dey $\textcolor{blue}{D}^{74}$, P. Di Nezza $\textcolor{blue}{D}^{26}$, I. Diachkov $\textcolor{blue}{D}^{42}$, S. Didenko $\textcolor{blue}{D}^{42}$, S. Ding $\textcolor{blue}{D}^{67}$, L. Dittmann $\textcolor{blue}{D}^{20}$, V. Dobishuk $\textcolor{blue}{D}^{51}$, A.D. Docheva $\textcolor{blue}{D}^{58}$, C. Dong $\textcolor{blue}{D}^4$, A.M. Donohoe $\textcolor{blue}{D}^{21}$, F. Dordei $\textcolor{blue}{D}^{30}$, A.C. dos Reis $\textcolor{blue}{D}^2$, A.D. Dowling $\textcolor{blue}{D}^{67}$, W. Duan $\textcolor{blue}{D}^{70}$, P. Duda $\textcolor{blue}{D}^{77}$, M.W. Dudek $\textcolor{blue}{D}^{39}$, L. Dufour $\textcolor{blue}{D}^{47}$, V. Duk $\textcolor{blue}{D}^{32}$, P. Durante $\textcolor{blue}{D}^{47}$, M.M. Duras $\textcolor{blue}{D}^{77}$, J.M. Durham $\textcolor{blue}{D}^{66}$, O.D. Durmus $\textcolor{blue}{D}^{74}$, A. Dziurda $\textcolor{blue}{D}^{39}$, A. Dzyuba $\textcolor{blue}{D}^{42}$, S. Easo $\textcolor{blue}{D}^{56}$, E. Eckstein $\textcolor{blue}{D}^{17}$, U. Egede $\textcolor{blue}{D}^1$, A. Egorychev $\textcolor{blue}{D}^{42}$, V. Egorychev $\textcolor{blue}{D}^{42}$, S. Eisenhardt $\textcolor{blue}{D}^{57}$, E. Ejopu $\textcolor{blue}{D}^{61}$, L. Eklund $\textcolor{blue}{D}^{79}$, M. Elashri $\textcolor{blue}{D}^{64}$, J. Ellbracht $\textcolor{blue}{D}^{18}$, S. Ely $\textcolor{blue}{D}^{60}$, A. Ene $\textcolor{blue}{D}^{41}$, E. Epple $\textcolor{blue}{D}^{64}$, J. Eschle $\textcolor{blue}{D}^{67}$, S. Esen $\textcolor{blue}{D}^{20}$, T. Evans $\textcolor{blue}{D}^{61}$, F. Fabiano $\textcolor{blue}{D}^{30,k}$, L.N. Falcao $\textcolor{blue}{D}^2$, Y. Fan $\textcolor{blue}{D}^7$, B. Fang $\textcolor{blue}{D}^{72}$, L. Fantini $\textcolor{blue}{D}^{32,r,47}$, M. Faria $\textcolor{blue}{D}^{48}$, K. Farmer $\textcolor{blue}{D}^{57}$, D. Fazzini $\textcolor{blue}{D}^{29,p}$, L. Felkowski $\textcolor{blue}{D}^{77}$, M. Feng $\textcolor{blue}{D}^{5,7}$, M. Feo $\textcolor{blue}{D}^{18,47}$, M. Fernandez Gomez $\textcolor{blue}{D}^{45}$, A.D. Fernez $\textcolor{blue}{D}^{65}$, F. Ferrari $\textcolor{blue}{D}^{23}$, F. Ferreira Rodrigues $\textcolor{blue}{D}^3$, M. Ferrillo $\textcolor{blue}{D}^{49}$, M. Ferro-Luzzi $\textcolor{blue}{D}^{47}$, S. Filippov $\textcolor{blue}{D}^{42}$, R.A. Fini $\textcolor{blue}{D}^{22}$, M. Fiorini $\textcolor{blue}{D}^{24,l}$, K.M. Fischer $\textcolor{blue}{D}^{62}$, D.S. Fitzgerald $\textcolor{blue}{D}^{80}$, C. Fitzpatrick $\textcolor{blue}{D}^{61}$, F. Fleuret $\textcolor{blue}{D}^{14}$, M. Fontana $\textcolor{blue}{D}^{23}$, L.F. Foreman $\textcolor{blue}{D}^{61}$, R. Forty $\textcolor{blue}{D}^{47}$, D. Foulds-Holt $\textcolor{blue}{D}^{54}$, M. Franco Sevilla $\textcolor{blue}{D}^{65}$, M. Frank $\textcolor{blue}{D}^{47}$, E. Franzoso $\textcolor{blue}{D}^{24,l}$, G. Frau $\textcolor{blue}{D}^{61}$, C. Frei $\textcolor{blue}{D}^{47}$, D.A. Friday $\textcolor{blue}{D}^{61}$, J. Fu $\textcolor{blue}{D}^7$, Q. Fuehring $\textcolor{blue}{D}^{18}$, Y. Fujii $\textcolor{blue}{D}^1$, T. Fulghesu $\textcolor{blue}{D}^{15}$, E. Gabriel $\textcolor{blue}{D}^{36}$, G. Galati $\textcolor{blue}{D}^{22}$, M.D. Galati $\textcolor{blue}{D}^{36}$, A. Gallas Torreira $\textcolor{blue}{D}^{45}$, D. Galli $\textcolor{blue}{D}^{23,j}$, S. Gambetta $\textcolor{blue}{D}^{57}$, M. Gandelman $\textcolor{blue}{D}^3$, P. Gandini $\textcolor{blue}{D}^{28}$, B. Ganie $\textcolor{blue}{D}^{61}$, H. Gao $\textcolor{blue}{D}^7$, R. Gao $\textcolor{blue}{D}^{62}$, Y. Gao $\textcolor{blue}{D}^8$, Y. Gao $\textcolor{blue}{D}^6$, Y. Gao $\textcolor{blue}{D}^8$, M. Garau $\textcolor{blue}{D}^{30,k}$, L.M. Garcia Martin $\textcolor{blue}{D}^{48}$, P. Garcia Moreno $\textcolor{blue}{D}^{44}$, J. García Pardiñas $\textcolor{blue}{D}^{47}$, K.G. Garg $\textcolor{blue}{D}^8$, L. Garrido $\textcolor{blue}{D}^{44}$, C. Gaspar $\textcolor{blue}{D}^{47}$, R.E. Geertsema $\textcolor{blue}{D}^{36}$, L.L. Gerken $\textcolor{blue}{D}^{18}$, E. Gersabeck $\textcolor{blue}{D}^{61}$, M. Gersabeck $\textcolor{blue}{D}^{61}$, T. Gershon $\textcolor{blue}{D}^{55}$, Z. Ghorbanimoghaddam $\textcolor{blue}{D}^{53}$, L. Giambastiani $\textcolor{blue}{D}^{31,q}$, F.I. Giasemis $\textcolor{blue}{D}^{15,e}$, V. Gibson $\textcolor{blue}{D}^{54}$, H.K. Giemza $\textcolor{blue}{D}^{40}$, A.L. Gilman $\textcolor{blue}{D}^{62}$, M. Giovannetti $\textcolor{blue}{D}^{26}$, A. Gioventù $\textcolor{blue}{D}^{44}$, P. Gironella Gironell $\textcolor{blue}{D}^{44}$, C. Giugliano $\textcolor{blue}{D}^{24,l}$, M.A. Giza $\textcolor{blue}{D}^{39}$, E.L. Gkougkousis $\textcolor{blue}{D}^{60}$, F.C. Glaser $\textcolor{blue}{D}^{13,20}$, V.V. Gligorov $\textcolor{blue}{D}^{15,47}$, C. Göbel $\textcolor{blue}{D}^{68}$, E. Golobardes $\textcolor{blue}{D}^{43}$, D. Golubkov $\textcolor{blue}{D}^{42}$, A. Golutvin $\textcolor{blue}{D}^{60,42,47}$, A. Gomes $\textcolor{blue}{D}^{2,a,\dagger}$, S. Gomez Fernandez $\textcolor{blue}{D}^{44}$, F. Goncalves Abrantes $\textcolor{blue}{D}^{62}$, M. Goncerz $\textcolor{blue}{D}^{39}$, G. Gong $\textcolor{blue}{D}^4$, J.A. Gooding $\textcolor{blue}{D}^{18}$, I.V. Gorelov $\textcolor{blue}{D}^{42}$, C. Gotti $\textcolor{blue}{D}^{29}$, J.P. Grabowski $\textcolor{blue}{D}^{17}$, L.A. Granado Cardoso $\textcolor{blue}{D}^{47}$, E. Graugés $\textcolor{blue}{D}^{44}$, E. Graverini $\textcolor{blue}{D}^{48,t}$, L. Grazette $\textcolor{blue}{D}^{55}$, G. Graziani $\textcolor{blue}{D}$, A.T. Grecu $\textcolor{blue}{D}^{41}$, L.M. Greeven $\textcolor{blue}{D}^{36}$, N.A. Grieser $\textcolor{blue}{D}^{64}$, L. Grillo $\textcolor{blue}{D}^{58}$, S. Gromov $\textcolor{blue}{D}^{42}$, C. Gu $\textcolor{blue}{D}^{14}$, M. Guarise $\textcolor{blue}{D}^{24}$, M. Guittiere $\textcolor{blue}{D}^{13}$, V. Guliaeva $\textcolor{blue}{D}^{42}$, P.A. Günther $\textcolor{blue}{D}^{20}$, A.-K. Guseinov $\textcolor{blue}{D}^{48}$, E. Gushchin $\textcolor{blue}{D}^{42}$, Y. Guz $\textcolor{blue}{D}^{6,42,47}$, T. Gys $\textcolor{blue}{D}^{47}$, K. Habermann $\textcolor{blue}{D}^{17}$, T. Hadavizadeh $\textcolor{blue}{D}^1$, C. Hadjivasilou $\textcolor{blue}{D}^{65}$, G. Haefeli $\textcolor{blue}{D}^{48}$, C. Haen $\textcolor{blue}{D}^{47}$, J. Haimberger $\textcolor{blue}{D}^{47}$, M. Hajheidari $\textcolor{blue}{D}^{47}$, M.M. Halvorsen $\textcolor{blue}{D}^{47}$, P.M. Hamilton $\textcolor{blue}{D}^{65}$, J. Hammerich $\textcolor{blue}{D}^{59}$, Q. Han $\textcolor{blue}{D}^8$, X. Han $\textcolor{blue}{D}^{20}$, S. Hansmann-Menzemer $\textcolor{blue}{D}^{20}$, L. Hao $\textcolor{blue}{D}^7$, N. Harnew $\textcolor{blue}{D}^{62}$, M. Hartmann $\textcolor{blue}{D}^{13}$, J. He $\textcolor{blue}{D}^{7,c}$, F. Hemmer $\textcolor{blue}{D}^{47}$, C. Henderson $\textcolor{blue}{D}^{64}$, R.D.L. Henderson $\textcolor{blue}{D}^{1,55}$, A.M. Hennequin $\textcolor{blue}{D}^{47}$, K. Hennessy $\textcolor{blue}{D}^{59}$, L. Henry $\textcolor{blue}{D}^{48}$, J. Herd $\textcolor{blue}{D}^{60}$, P. Herrero Gascon $\textcolor{blue}{D}^{20}$, J. Heuel $\textcolor{blue}{D}^{16}$, A. Hicheur $\textcolor{blue}{D}^3$, G. Hijano Mendizabal $\textcolor{blue}{D}^{49}$, D. Hill $\textcolor{blue}{D}^{48}$, S.E. Hollitt $\textcolor{blue}{D}^{18}$, J. Horswill $\textcolor{blue}{D}^{61}$, R. Hou $\textcolor{blue}{D}^8$, Y. Hou $\textcolor{blue}{D}^{11}$, N. Howarth $\textcolor{blue}{D}^{59}$, J. Hu $\textcolor{blue}{D}^{20}$, J. Hu $\textcolor{blue}{D}^{70}$, W. Hu $\textcolor{blue}{D}^6$, X. Hu $\textcolor{blue}{D}^4$, W. Huang $\textcolor{blue}{D}^7$, W. Hulsbergen $\textcolor{blue}{D}^{36}$, R.J. Hunter $\textcolor{blue}{D}^{55}$, M. Hushchyn $\textcolor{blue}{D}^{42}$, D. Hutchcroft $\textcolor{blue}{D}^{59}$, D. Ilin $\textcolor{blue}{D}^{42}$, P. Ilten $\textcolor{blue}{D}^{64}$, A. Inglessi $\textcolor{blue}{D}^{42}$, A. Iniuksu $\textcolor{blue}{D}^{42}$, A. Ishteev $\textcolor{blue}{D}^{42}$, K. Ivshin $\textcolor{blue}{D}^{42}$, R. Jacobsson $\textcolor{blue}{D}^{47}$, H. Jage $\textcolor{blue}{D}^{16}$, S.J. Jaimes Elles $\textcolor{blue}{D}^{46,73}$, S. Jakobsen $\textcolor{blue}{D}^{47}$, E. Jans $\textcolor{blue}{D}^{36}$, B.K. Jashal $\textcolor{blue}{D}^{46}$, A. Jawahery $\textcolor{blue}{D}^{65,47}$,

- V. Jevtic ID^{18} , E. Jiang ID^{65} , X. Jiang $\text{ID}^{5,7}$, Y. Jiang ID^7 , Y.J. Jiang ID^6 , M. John ID^{62} , D. Johnson ID^{52} , C.R. Jones ID^{54} , T.P. Jones ID^{55} , S. Joshi ID^{40} , B. Jost ID^{47} , N. Jurik ID^{47} , I. Juszczak ID^{39} , D. Kaminaris ID^{48} , S. Kandybei ID^{50} , Y. Kang ID^4 , C. Kar ID^{11} , M. Karacson ID^{47} , D. Karpenkov ID^{42} , A. Kauniskangas ID^{48} , J.W. Kautz ID^{64} , F. Keizer ID^{47} , M. Kenzie ID^{54} , T. Ketel ID^{36} , B. Khanji ID^{67} , A. Kharisova ID^{42} , S. Kholodenko $\text{ID}^{33,47}$, G. Khreich ID^{13} , T. Kirn ID^{16} , V.S. Kirsebom $\text{ID}^{29,p}$, O. Kitouni ID^{63} , S. Klaver ID^{37} , N. Kleijne $\text{ID}^{33,s}$, K. Klimaszewski ID^{40} , M.R. Kmiec ID^{40} , S. Koliiev ID^{51} , L. Kolk ID^{18} , A. Konoplyannikov ID^{42} , P. Kopciewicz $\text{ID}^{38,47}$, P. Koppenburg ID^{36} , M. Korolev ID^{42} , I. Kostiuk ID^{36} , O. Kot ID^{51} , S. Kotriakhova ID , A. Kozachuk ID^{42} , P. Kravchenko ID^{42} , L. Kravchuk ID^{42} , M. Kreps ID^{55} , P. Krokovny ID^{42} , W. Krupa ID^{67} , W. Krzemien ID^{40} , O.K. Kshyvanskyi ID^{51} , J. Kubat ID^{20} , S. Kubis ID^{77} , M. Kucharczyk ID^{39} , V. Kudryavtsev ID^{42} , E. Kulikova ID^{42} , A. Kupsc ID^{79} , B.K. Kutsenko ID^{12} , D. Lacarrere ID^{47} , A. Lai ID^{30} , A. Lampis ID^{30} , D. Lancierini ID^{54} , C. Landesa Gomez ID^{45} , J.J. Lane ID^1 , R. Lane ID^{53} , C. Langenbruch ID^{20} , J. Langer ID^{18} , O. Lantwin ID^{42} , T. Latham ID^{55} , F. Lazzari $\text{ID}^{33,t}$, C. Lazzeroni ID^{52} , R. Le Gac ID^{12} , R. Lefèvre ID^{11} , A. Leflat ID^{42} , S. Legotin ID^{42} , M. Lehuraux ID^{55} , E. Lemos Cid ID^{47} , O. Leroy ID^{12} , T. Lesiak ID^{39} , B. Leverington ID^{20} , A. Li ID^4 , H. Li ID^{70} , K. Li ID^8 , L. Li ID^{61} , P. Li ID^{47} , P.-R. Li ID^{71} , Q. Li $\text{ID}^{5,7}$, S. Li ID^8 , T. Li $\text{ID}^{5,d}$, T. Li ID^{70} , Y. Li ID^8 , Y. Li ID^5 , Z. Lian ID^4 , X. Liang ID^{67} , S. Libralon ID^{46} , C. Lin ID^7 , T. Lin ID^{56} , R. Lindner ID^{47} , V. Lisovskyi ID^{48} , R. Litvinov $\text{ID}^{30,47}$, F.L. Liu ID^1 , G. Liu ID^{70} , K. Liu ID^{71} , S. Liu $\text{ID}^{5,7}$, Y. Liu ID^{57} , Y. Liu ID^{71} , Y.L. Liu ID^{60} , A. Lobo Salvia ID^{44} , A. Loi ID^{30} , J. Lomba Castro ID^{45} , T. Long ID^{54} , J.H. Lopes ID^3 , A. Lopez Huertas ID^{44} , S. López Soliño ID^{45} , C. Lucarelli $\text{ID}^{25,m}$, D. Lucchesi $\text{ID}^{31,q}$, M. Lucio Martinez ID^{76} , V. Lukashenko $\text{ID}^{36,51}$, Y. Luo ID^6 , A. Lupato ID^{31} , E. Luppi $\text{ID}^{24,l}$, K. Lynch ID^{21} , X.-R. Lyu ID^7 , G.M. Ma ID^4 , R. Ma ID^7 , S. Maccolini ID^{18} , F. Machefert ID^{13} , F. Maciuc ID^{41} , B. Mack ID^{67} , I. Mackay ID^{62} , L.M. Mackey ID^{67} , L.R. Madhan Mohan ID^{54} , M.M. Madurai ID^{52} , A. Maevskiy ID^{42} , D. Magdalinski ID^{36} , D. Maisuzenko ID^{42} , M.W. Majewski ID^{38} , J.J. Malczewski ID^{39} , S. Malde ID^{62} , L. Malentacca ID^{47} , A. Malinin ID^{42} , T. Maltsev ID^{42} , G. Manca $\text{ID}^{30,k}$, G. Mancinelli ID^{12} , C. Mancuso $\text{ID}^{28,13,o}$, R. Manera Escalero ID^{44} , D. Manuzzi ID^{23} , D. Marangotto $\text{ID}^{28,o}$, J.F. Marchand ID^{10} , R. Marchevski ID^{48} , U. Marconi ID^{23} , S. Mariani ID^{47} , C. Marin Benito ID^{44} , J. Marks ID^{20} , A.M. Marshall ID^{53} , G. Martelli $\text{ID}^{32,r}$, G. Martellotti ID^{34} , L. Martinazzoli ID^{47} , M. Martinelli $\text{ID}^{29,p}$, D. Martinez Santos ID^{45} , F. Martinez Vidal ID^{46} , A. Massafferri ID^2 , R. Matev ID^{47} , A. Mathad ID^{47} , V. Matiunin ID^{42} , C. Matteuzzi ID^{67} , K.R. Mattioli ID^{14} , A. Mauri ID^{60} , E. Maurice ID^{14} , J. Mauricio ID^{44} , P. Mayencourt ID^{48} , M. Mazurek ID^{40} , M. McCann ID^{60} , L. McConnell ID^{21} , T.H. McGrath ID^{61} , N.T. McHugh ID^{58} , A. McNab ID^{61} , R. McNulty ID^{21} , B. Meadows ID^{64} , G. Meier ID^{18} , D. Melnychuk ID^{40} , F.M. Meng ID^4 , M. Merk $\text{ID}^{36,76}$, A. Merli ID^{48} , L. Meyer Garcia ID^{65} , D. Miao $\text{ID}^{5,7}$, H. Miao ID^7 , M. Mikhasenko $\text{ID}^{17,f}$, D.A. Milanes ID^{73} , A. Minotti $\text{ID}^{29,p}$, E. Minucci ID^{67} , T. Miralles ID^{11} , B. Mitreska ID^{18} , D.S. Mitzel ID^{18} , A. Modak ID^{56} , A. Mödden ID^{18} , R.A. Mohammed ID^{62} , R.D. Moise ID^{16} , S. Mokhnenko ID^{42} , T. Mombächer ID^{47} , M. Monk $\text{ID}^{55,1}$, S. Monteil ID^{11} , A. Morcillo Gomez ID^{45} , G. Morello ID^{26} , M.J. Morello $\text{ID}^{33,s}$, M.P. Morgenthaler ID^{20} , A.B. Morris ID^{47} , A.G. Morris ID^{12} , R. Mountain ID^{67} , H. Mu ID^4 , Z.M. Mu ID^6 , E. Muhammad ID^{55} , F. Muheim ID^{57} , M. Mulder ID^{75} , K. Müller ID^{49} , F. Muñoz-Rojas ID^9 , R. Murta ID^{60} , P. Naik ID^{59} , T. Nakada ID^{48} , R. Nandakumar ID^{56} , T. Nanut ID^{47} , I. Nasteva ID^3 , M. Needham ID^{57} , N. Neri $\text{ID}^{28,o}$, S. Neubert ID^{17} , N. Neufeld ID^{47} , P. Neustroev ID^{42} , J. Nicolini $\text{ID}^{18,13}$, D. Nicotra ID^{76} , E.M. Niel ID^{48} , N. Nikitin ID^{42} , P. Nogarolli ID^3 , P. Nogga ID^{17} , N.S. Nolte ID^{63} , C. Normand ID^{53} , J. Novoa Fernandez ID^{45} , G. Nowak ID^{64} , C. Nunez ID^{80} , H.N. Nur ID^{58} , A. Oblakowska-Mucha ID^{38} , V. Obraztsov ID^{42} ,

- T. Oeser ID^{16} , S. Okamura $\text{ID}^{24,l}$, A. Okhotnikov ID^{42} , O. Okhrimenko ID^{51} , R. Oldeman $\text{ID}^{30,k}$,
 F. Oliva ID^{57} , M. Olocco ID^{18} , C.J.G. Onderwater ID^{76} , R.H. O’Neil ID^{57} , J.M. Otalora Goicochea ID^3 ,
 P. Owen ID^{49} , A. Oyanguren ID^{46} , O. Ozcelik ID^{57} , K.O. Paddeken ID^{17} , B. Pagare ID^{55} , P.R. Pais ID^{20} ,
 T. Pajero ID^{47} , A. Palano ID^{22} , M. Palutan ID^{26} , G. Panshin ID^{42} , L. Paolucci ID^{55} , A. Papanestis ID^{56} ,
 M. Pappagallo $\text{ID}^{22,h}$, L.L. Pappalardo $\text{ID}^{24,l}$, C. Pappenheimer ID^{64} , C. Parkes ID^{61} , B. Passalacqua ID^{24} ,
 G. Passaleva ID^{25} , D. Passaro $\text{ID}^{33,s}$, A. Pastore ID^{22} , M. Patel ID^{60} , J. Patoc ID^{62} , C. Patrignani $\text{ID}^{23,j}$,
 A. Paul ID^{67} , C.J. Pawley ID^{76} , A. Pellegrino ID^{36} , J. Peng $\text{ID}^{5,7}$, M. Pepe Altarelli ID^{26} , S. Perazzini ID^{23} ,
 D. Pereima ID^{42} , H. Pereira Da Costa ID^{66} , A. Pereiro Castro ID^{45} , P. Perret ID^{11} , A. Perro ID^{47} ,
 K. Petridis ID^{53} , A. Petrolini $\text{ID}^{27,n}$, J.P. Pfaller ID^{64} , H. Pham ID^{67} , L. Pica ID^{33} , M. Piccini ID^{32} ,
 B. Pietrzyk ID^{10} , G. Pietrzyk ID^{13} , D. Pinci ID^{34} , F. Pisani ID^{47} , M. Pizzichemi $\text{ID}^{29,p}$, V. Placinta ID^{41} ,
 M. Plo Casasus ID^{45} , F. Polci $\text{ID}^{15,47}$, M. Poli Lener ID^{26} , A. Poluektov ID^{12} , N. Polukhina ID^{42} ,
 I. Polyakov ID^{47} , E. Polycarpo ID^3 , S. Ponce ID^{47} , D. Popov ID^7 , S. Poslavskii ID^{42} , K. Prasanth ID^{57} ,
 C. Prouve ID^{45} , V. Pugatch ID^{51} , G. Punzi $\text{ID}^{33,t}$, S. Qasim ID^{49} , Q.Q. Qian ID^6 , W. Qian ID^7 , N. Qin ID^4 ,
 S. Qu ID^4 , R. Quagliani ID^{47} , R.I. Rabadan Trejo ID^{55} , J.H. Rademacker ID^{53} , M. Rama ID^{33} ,
 M. Ramírez García ID^{80} , V. Ramos De Oliveira ID^{68} , M. Ramos Pernas ID^{55} , M.S. Rangel ID^3 ,
 F. Ratnikov ID^{42} , G. Raven ID^{37} , M. Rebollo De Miguel ID^{46} , F. Redi $\text{ID}^{28,i}$, J. Reich ID^{53} , F. Reiss ID^{61} ,
 Z. Ren ID^7 , P.K. Resmi ID^{62} , R. Ribatti ID^{48} , G.R. Ricart $\text{ID}^{14,81}$, D. Riccardi $\text{ID}^{33,s}$, S. Ricciardi ID^{56} ,
 K. Richardson ID^{63} , M. Richardson-Slipper ID^{57} , K. Rinnert ID^{59} , P. Robbe ID^{13} , G. Robertson ID^{58} ,
 E. Rodrigues ID^{59} , E. Rodriguez Fernandez ID^{45} , J.A. Rodriguez Lopez ID^{73} ,
 E. Rodriguez Rodriguez ID^{45} , A. Rogovskiy ID^{56} , D.L. Rolf ID^{47} , P. Roloff ID^{47} , V. Romanovskiy ID^{42} ,
 M. Romero Lamas ID^{45} , A. Romero Vidal ID^{45} , G. Romolini ID^{24} , F. Ronchetti ID^{48} , T. Rong ID^6 ,
 M. Rotondo ID^{26} , S.R. Roy ID^{20} , M.S. Rudolph ID^{67} , T. Ruf ID^{47} , M. Ruiz Diaz ID^{20} ,
 R.A. Ruiz Fernandez ID^{45} , J. Ruiz Vidal $\text{ID}^{79,aa}$, A. Ryzhikov ID^{42} , J. Ryzka ID^{38} ,
 J.J. Saavedra-Arias ID^9 , J.J. Saborido Silva ID^{45} , R. Sadek ID^{14} , N. Sagidova ID^{42} , D. Sahoo ID^{74} ,
 N. Sahoo ID^{52} , B. Saitta $\text{ID}^{30,k}$, M. Salomoni $\text{ID}^{29,p,47}$, C. Sanchez Gras ID^{36} , I. Sanderswood ID^{46} ,
 R. Santacesaria ID^{34} , C. Santamarina Rios ID^{45} , M. Santimaria $\text{ID}^{26,47}$, L. Santoro ID^2 , E. Santovetti ID^{35} ,
 A. Saputi $\text{ID}^{24,47}$, D. Saranin ID^{42} , A.S. Sarnatskiy ID^{75} , G. Sarpis ID^{57} , M. Sarpis ID^{61} , C. Satriano $\text{ID}^{34,u}$,
 A. Satta ID^{35} , M. Saur ID^6 , D. Savrina ID^{42} , H. Sazak ID^{16} , L.G. Scantlebury Smead ID^{62} ,
 A. Scarabotto ID^{18} , S. Schael ID^{16} , S. Scherl ID^{59} , M. Schiller ID^{58} , H. Schindler ID^{47} , M. Schmelling ID^{19} ,
 B. Schmidt ID^{47} , S. Schmitt ID^{16} , H. Schmitz ID^{17} , O. Schneider ID^{48} , A. Schopper ID^{47} , N. Schulte ID^{18} ,
 S. Schulte ID^{48} , M.H. Schune ID^{13} , R. Schwemmer ID^{47} , G. Schwering ID^{16} , B. Sciascia ID^{26} ,
 A. Sciuccati ID^{47} , S. Sellam ID^{45} , A. Semennikov ID^{42} , T. Senger ID^{49} , M. Senghi Soares ID^{37} ,
 A. Sergi ID^{27} , N. Serra ID^{49} , L. Sestini ID^{31} , A. Seuthe ID^{18} , Y. Shang ID^6 , D.M. Shangase ID^{80} ,
 M. Shapkin ID^{42} , R.S. Sharma ID^{67} , I. Shchemberov ID^{42} , L. Shchutska ID^{48} , T. Shears ID^{59} ,
 L. Shekhtman ID^{42} , Z. Shen ID^6 , S. Sheng $\text{ID}^{5,7}$, V. Shevchenko ID^{42} , B. Shi ID^7 , Q. Shi ID^7 ,
 Y. Shimizu ID^{13} , E. Shmanin ID^{42} , R. Shorkin ID^{42} , J.D. Shupperd ID^{67} , R. Silva Coutinho ID^{67} ,
 G. Simi $\text{ID}^{31,q}$, S. Simone $\text{ID}^{22,h}$, N. Skidmore ID^{55} , T. Skwarnicki ID^{67} , M.W. Slater ID^{52} ,
 J.C. Smallwood ID^{62} , E. Smith ID^{63} , K. Smith ID^{66} , M. Smith ID^{60} , A. Snoch ID^{36} , L. Soares Lavra ID^{57} ,
 M.D. Sokoloff ID^{64} , F.J.P. Soler ID^{58} , A. Solomin $\text{ID}^{42,53}$, A. Solovev ID^{42} , I. Solovyev ID^{42} , R. Song ID^1 ,
 Y. Song ID^{48} , Y. Song ID^4 , Y.S. Song ID^6 , F.L. Souza De Almeida ID^{67} , B. Souza De Paula ID^3 ,
 E. Spadaro Norella $\text{ID}^{28,o}$, E. Spedicato ID^{23} , J.G. Speer ID^{18} , E. Spiridenkov ID^{42} , P. Spradlin ID^{58} ,
 V. Sriskaran ID^{47} , F. Stagni ID^{47} , M. Stahl ID^{47} , S. Stahl ID^{47} , S. Stanislaus ID^{62} , E.N. Stein ID^{47} ,
 O. Steinkamp ID^{49} , O. Stenyakin ID^{42} , H. Stevens ID^{18} , D. Strekalina ID^{42} , Y. Su ID^7 , F. Suljik ID^{62} ,

- J. Sun ¹⁰³⁰, L. Sun ¹⁰⁷², Y. Sun ¹⁰⁶⁵, D.S. Sundfeld Lima², W. Sutcliffe⁴⁹, P.N. Swallow ¹⁰⁵², F. Swystun ¹⁰⁵⁴, A. Szabelski ¹⁰⁴⁰, T. Szumlak ¹⁰³⁸, Y. Tan ¹⁰⁴, M.D. Tat ¹⁰⁶², A. Terentev ¹⁰⁴², F. Terzuoli ¹⁰^{33,w,47}, F. Teubert ¹⁰⁴⁷, E. Thomas ¹⁰⁴⁷, D.J.D. Thompson ¹⁰⁵², H. Tilquin ¹⁰⁶⁰, V. Tisserand ¹⁰¹¹, S. T'Jampens ¹⁰¹⁰, M. Tobin ¹⁰^{5,47}, L. Tomassetti ¹⁰^{24,l}, G. Tonani ¹⁰^{28,o,47}, X. Tong ¹⁰⁶, D. Torres Machado ¹⁰², L. Toscano ¹⁰¹⁸, D.Y. Tou ¹⁰⁴, C. Trippl ¹⁰⁴³, G. Tuci ¹⁰²⁰, N. Tuning ¹⁰³⁶, L.H. Uecker ¹⁰²⁰, A. Ukleja ¹⁰³⁸, D.J. Unverzagt ¹⁰²⁰, E. Ursov ¹⁰⁴², A. Usachov ¹⁰³⁷, A. Ustyuzhanin ¹⁰⁴², U. Uwer ¹⁰²⁰, V. Vagnoni ¹⁰²³, G. Valenti ¹⁰²³, N. Valls Canudas ¹⁰⁴⁷, H. Van Hecke ¹⁰⁶⁶, E. van Herwijnen ¹⁰⁶⁰, C.B. Van Hulse ¹⁰^{45,y}, R. Van Laak ¹⁰⁴⁸, M. van Veghel ¹⁰³⁶, G. Vasquez ¹⁰⁴⁹, R. Vazquez Gomez ¹⁰⁴⁴, P. Vazquez Regueiro ¹⁰⁴⁵, C. Vázquez Sierra ¹⁰⁴⁵, S. Vecchi ¹⁰²⁴, J.J. Velthuis ¹⁰⁵³, M. Veltri ¹⁰^{25,x}, A. Venkateswaran ¹⁰⁴⁸, M. Vesterinen ¹⁰⁵⁵, M. Vieites Diaz ¹⁰⁴⁷, X. Vilasis-Cardona ¹⁰⁴³, E. Vilella Figueras ¹⁰⁵⁹, A. Villa ¹⁰²³, P. Vincent ¹⁰¹⁵, F.C. Volle ¹⁰⁵², D. vom Bruch ¹⁰¹², N. Voropaev ¹⁰⁴², K. Vos ¹⁰⁷⁶, G. Vouters ¹⁰^{10,47}, C. Vrahas ¹⁰⁵⁷, J. Wagner ¹⁰¹⁸, J. Walsh ¹⁰³³, E.J. Walton ¹⁰^{1,55}, G. Wan ¹⁰⁶, C. Wang ¹⁰²⁰, G. Wang ¹⁰⁸, J. Wang ¹⁰⁶, J. Wang ¹⁰⁵, J. Wang ¹⁰⁴, J. Wang ¹⁰⁷², M. Wang ¹⁰²⁸, N.W. Wang ¹⁰⁷, R. Wang ¹⁰⁵³, X. Wang ⁸, X. Wang ¹⁰⁷⁰, X.W. Wang ¹⁰⁶⁰, Y. Wang ¹⁰⁶, Z. Wang ¹⁰¹³, Z. Wang ¹⁰⁴, Z. Wang ¹⁰²⁸, J.A. Ward ¹⁰^{55,1}, M. Waterlaat ⁴⁷, N.K. Watson ¹⁰⁵², D. Websdale ¹⁰⁶⁰, Y. Wei ¹⁰⁶, J. Wendel ¹⁰⁷⁸, B.D.C. Westhenry ¹⁰⁵³, D.J. White ¹⁰⁶¹, M. Whitehead ¹⁰⁵⁸, A.R. Wiederhold ¹⁰⁵⁵, D. Wiedner ¹⁰¹⁸, G. Wilkinson ¹⁰⁶², M.K. Wilkinson ¹⁰⁶⁴, M. Williams ¹⁰⁶³, M.R.J. Williams ¹⁰⁵⁷, R. Williams ¹⁰⁵⁴, F.F. Wilson ¹⁰⁵⁶, W. Wislicki ¹⁰⁴⁰, M. Witek ¹⁰³⁹, L. Witola ¹⁰²⁰, C.P. Wong ¹⁰⁶⁶, G. Wormser ¹⁰¹³, S.A. Wotton ¹⁰⁵⁴, H. Wu ¹⁰⁶⁷, J. Wu ¹⁰⁸, Y. Wu ¹⁰⁶, K. Wyllie ¹⁰⁴⁷, S. Xian ⁷⁰, Z. Xiang ¹⁰⁵, Y. Xie ¹⁰⁸, A. Xu ¹⁰³³, J. Xu ¹⁰⁷, L. Xu ¹⁰⁴, L. Xu ¹⁰⁴, M. Xu ¹⁰⁵⁵, Z. Xu ¹⁰¹¹, Z. Xu ¹⁰⁷, Z. Xu ¹⁰⁵, D. Yang ¹⁰⁴, K. Yang ¹⁰⁶⁰, S. Yang ¹⁰⁷, X. Yang ¹⁰⁶, Y. Yang ¹⁰^{27,n}, Z. Yang ¹⁰⁶, Z. Yang ¹⁰⁶⁵, V. Yeroshenko ¹⁰¹³, H. Yeung ¹⁰⁶¹, H. Yin ¹⁰⁸, C.Y. Yu ¹⁰⁶, J. Yu ¹⁰⁶⁹, X. Yuan ¹⁰⁵, E. Zaffaroni ¹⁰⁴⁸, M. Zavertyaev ¹⁰¹⁹, M. Zdybal ¹⁰³⁹, C. Zeng ¹⁰^{5,7}, M. Zeng ¹⁰⁴, C. Zhang ¹⁰⁶, D. Zhang ¹⁰⁸, J. Zhang ¹⁰⁷, L. Zhang ¹⁰⁴, S. Zhang ¹⁰⁶⁹, S. Zhang ¹⁰⁶, Y. Zhang ¹⁰⁶, Y.Z. Zhang ¹⁰⁴, Y. Zhao ¹⁰²⁰, A. Zharkova ¹⁰⁴², A. Zhelezov ¹⁰²⁰, S.Z. Zheng ⁶, X.Z. Zheng ¹⁰⁴, Y. Zheng ¹⁰⁷, T. Zhou ¹⁰⁶, X. Zhou ¹⁰⁸, Y. Zhou ¹⁰⁷, V. Zhokovska ¹⁰⁵⁵, L.Z. Zhu ¹⁰⁷, X. Zhu ¹⁰⁴, X. Zhu ¹⁰⁸, V. Zhukov ¹⁰¹⁶, J. Zhuo ¹⁰⁴⁶, Q. Zou ¹⁰^{5,7}, D. Zuliani ¹⁰^{31,q}, G. Zunică ¹⁰⁴⁸

¹ School of Physics and Astronomy, Monash University, Melbourne, Australia² Centro Brasileiro de Pesquisas Físicas (CBPF), Rio de Janeiro, Brazil³ Universidade Federal do Rio de Janeiro (UFRJ), Rio de Janeiro, Brazil⁴ Center for High Energy Physics, Tsinghua University, Beijing, China⁵ Institute Of High Energy Physics (IHEP), Beijing, China⁶ School of Physics State Key Laboratory of Nuclear Physics and Technology, Peking University, Beijing, China⁷ University of Chinese Academy of Sciences, Beijing, China⁸ Institute of Particle Physics, Central China Normal University, Wuhan, Hubei, China⁹ Consejo Nacional de Rectores (CONARE), San Jose, Costa Rica¹⁰ Université Savoie Mont Blanc, CNRS, IN2P3-LAPP, Annecy, France¹¹ Université Clermont Auvergne, CNRS/IN2P3, LPC, Clermont-Ferrand, France¹² Aix Marseille Univ, CNRS/IN2P3, CPPM, Marseille, France¹³ Université Paris-Saclay, CNRS/IN2P3, IJCLab, Orsay, France¹⁴ Laboratoire Leprince-Ringuet, CNRS/IN2P3, Ecole Polytechnique, Institut Polytechnique de Paris, Palaiseau, France¹⁵ LPNHE, Sorbonne Université, Paris Diderot Sorbonne Paris Cité, CNRS/IN2P3, Paris, France¹⁶ I. Physikalisches Institut, RWTH Aachen University, Aachen, Germany

- ¹⁷ Universität Bonn - Helmholtz-Institut für Strahlen und Kernphysik, Bonn, Germany
¹⁸ Fakultät Physik, Technische Universität Dortmund, Dortmund, Germany
¹⁹ Max-Planck-Institut für Kernphysik (MPIK), Heidelberg, Germany
²⁰ Physikalisches Institut, Ruprecht-Karls-Universität Heidelberg, Heidelberg, Germany
²¹ School of Physics, University College Dublin, Dublin, Ireland
²² INFN Sezione di Bari, Bari, Italy
²³ INFN Sezione di Bologna, Bologna, Italy
²⁴ INFN Sezione di Ferrara, Ferrara, Italy
²⁵ INFN Sezione di Firenze, Firenze, Italy
²⁶ INFN Laboratori Nazionali di Frascati, Frascati, Italy
²⁷ INFN Sezione di Genova, Genova, Italy
²⁸ INFN Sezione di Milano, Milano, Italy
²⁹ INFN Sezione di Milano-Bicocca, Milano, Italy
³⁰ INFN Sezione di Cagliari, Monserrato, Italy
³¹ INFN Sezione di Padova, Padova, Italy
³² INFN Sezione di Perugia, Perugia, Italy
³³ INFN Sezione di Pisa, Pisa, Italy
³⁴ INFN Sezione di Roma La Sapienza, Roma, Italy
³⁵ INFN Sezione di Roma Tor Vergata, Roma, Italy
³⁶ Nikhef National Institute for Subatomic Physics, Amsterdam, The Netherlands
³⁷ Nikhef National Institute for Subatomic Physics and VU University Amsterdam, Amsterdam, The Netherlands
³⁸ AGH - University of Krakow, Faculty of Physics and Applied Computer Science, Kraków, Poland
³⁹ Henryk Niewodniczanski Institute of Nuclear Physics Polish Academy of Sciences, Kraków, Poland
⁴⁰ National Center for Nuclear Research (NCBJ), Warsaw, Poland
⁴¹ Horia Hulubei National Institute of Physics and Nuclear Engineering, Bucharest-Magurele, Romania
⁴² Affiliated with an institute covered by a cooperation agreement with CERN
⁴³ DS4DS, La Salle, Universitat Ramon Llull, Barcelona, Spain
⁴⁴ ICCUB, Universitat de Barcelona, Barcelona, Spain
⁴⁵ Instituto Galego de Física de Altas Enerxías (IGFAE), Universidade de Santiago de Compostela, Santiago de Compostela, Spain
⁴⁶ Instituto de Fisica Corpuscular, Centro Mixto Universidad de Valencia - CSIC, Valencia, Spain
⁴⁷ European Organization for Nuclear Research (CERN), Geneva, Switzerland
⁴⁸ Institute of Physics, Ecole Polytechnique Fédérale de Lausanne (EPFL), Lausanne, Switzerland
⁴⁹ Physik-Institut, Universität Zürich, Zürich, Switzerland
⁵⁰ NSC Kharkiv Institute of Physics and Technology (NSC KIPT), Kharkiv, Ukraine
⁵¹ Institute for Nuclear Research of the National Academy of Sciences (KINR), Kyiv, Ukraine
⁵² University of Birmingham, Birmingham, United Kingdom
⁵³ H.H. Wills Physics Laboratory, University of Bristol, Bristol, United Kingdom
⁵⁴ Cavendish Laboratory, University of Cambridge, Cambridge, United Kingdom
⁵⁵ Department of Physics, University of Warwick, Coventry, United Kingdom
⁵⁶ STFC Rutherford Appleton Laboratory, Didcot, United Kingdom
⁵⁷ School of Physics and Astronomy, University of Edinburgh, Edinburgh, United Kingdom
⁵⁸ School of Physics and Astronomy, University of Glasgow, Glasgow, United Kingdom
⁵⁹ Oliver Lodge Laboratory, University of Liverpool, Liverpool, United Kingdom
⁶⁰ Imperial College London, London, United Kingdom
⁶¹ Department of Physics and Astronomy, University of Manchester, Manchester, United Kingdom
⁶² Department of Physics, University of Oxford, Oxford, United Kingdom
⁶³ Massachusetts Institute of Technology, Cambridge, MA, United States
⁶⁴ University of Cincinnati, Cincinnati, OH, United States
⁶⁵ University of Maryland, College Park, MD, United States
⁶⁶ Los Alamos National Laboratory (LANL), Los Alamos, NM, United States
⁶⁷ Syracuse University, Syracuse, NY, United States

- ⁶⁸ Pontifícia Universidade Católica do Rio de Janeiro (PUC-Rio), Rio de Janeiro, Brazil, associated to³
- ⁶⁹ School of Physics and Electronics, Hunan University, Changsha City, China, associated to⁸
- ⁷⁰ Guangdong Provincial Key Laboratory of Nuclear Science, Guangdong-Hong Kong Joint Laboratory of Quantum Matter, Institute of Quantum Matter, South China Normal University, Guangzhou, China, associated to⁴
- ⁷¹ Lanzhou University, Lanzhou, China, associated to⁵
- ⁷² School of Physics and Technology, Wuhan University, Wuhan, China, associated to⁴
- ⁷³ Departamento de Fisica, Universidad Nacional de Colombia, Bogota, Colombia, associated to¹⁵
- ⁷⁴ Eotvos Lorand University, Budapest, Hungary, associated to⁴⁷
- ⁷⁵ Van Swinderen Institute, University of Groningen, Groningen, The Netherlands, associated to³⁶
- ⁷⁶ Universiteit Maastricht, Maastricht, The Netherlands, associated to³⁶
- ⁷⁷ Tadeusz Kosciuszko Cracow University of Technology, Cracow, Poland, associated to³⁹
- ⁷⁸ Universidad da Coruña, A Coruna, Spain, associated to⁴³
- ⁷⁹ Department of Physics and Astronomy, Uppsala University, Uppsala, Sweden, associated to⁵⁸
- ⁸⁰ University of Michigan, Ann Arbor, MI, United States, associated to⁶⁷
- ⁸¹ Departement de Physique Nucleaire (SPhN), Gif-Sur-Yvette, France

^a Universidade de Brasília, Brasília, Brazil

^b Centro Federal de Educacão Tecnológica Celso Suckow da Fonseca, Rio De Janeiro, Brazil

^c Hangzhou Institute for Advanced Study, UCAS, Hangzhou, China

^d School of Physics and Electronics, Henan University, Kaifeng, China

^e LIP6, Sorbonne Universite, Paris, France

^f Excellence Cluster ORIGINS, Munich, Germany

^g Universidad Nacional Autónoma de Honduras, Tegucigalpa, Honduras

^h Università di Bari, Bari, Italy

ⁱ Università degli studi di Bergamo, Bergamo, Italy

^j Università di Bologna, Bologna, Italy

^k Università di Cagliari, Cagliari, Italy

^l Università di Ferrara, Ferrara, Italy

^m Università di Firenze, Firenze, Italy

ⁿ Università di Genova, Genova, Italy

^o Università degli Studi di Milano, Milano, Italy

^p Università degli Studi di Milano-Bicocca, Milano, Italy

^q Università di Padova, Padova, Italy

^r Università di Perugia, Perugia, Italy

^s Scuola Normale Superiore, Pisa, Italy

^t Università di Pisa, Pisa, Italy

^u Università della Basilicata, Potenza, Italy

^v Università di Roma Tor Vergata, Roma, Italy

^w Università di Siena, Siena, Italy

^x Università di Urbino, Urbino, Italy

^y Universidad de Alcalá, Alcalá de Henares, Spain

^z Facultad de Ciencias Fisicas, Madrid, Spain

^{aa} Department of Physics/Division of Particle Physics, Lund, Sweden

[†] Deceased